# Long non-coding RNA 01614 hyperactivates WNT/β-catenin signaling to promote pancreatic cancer progression by suppressing GSK-3β

LONG-JIANG CHEN[1,2*], LUN WU[3*], WEI WANG[1,2], LU-LU ZHAI[1], FENG XIANG[1], WEI-BO LI[1] and ZHI-GANG TANG[1,2]

[1]Department of Pancreatic Surgery, and [2]Key Laboratory of Hubei Province for Digestive System Disease, Renmin Hospital of Wuhan University, Wuhan, Hubei 430060; [3]Department of Breast and Thyroid Surgery, Experiment Center of Medicine, Sinopharm Dongfeng General Hospital, Hubei University of Medicine, Shiyan, Hubei 442008, P.R. China

Received March 10, 2022; Accepted June 24, 2022

DOI: 10.3892/ijo.2022.5406

**Abstract.** Pancreatic cancer (PC) is a lethal type of cancer for which effective therapies are limited. Long non-coding RNAs (lncRNAs) represent a critical type of regulator category, mediating the tumorigenesis and development of various tumor types, including PC. However, the expression patterns and functions of numerous lncRNAs in PC remain poorly understood. In the present study, linc01614 was identified as a PC-related lncRNA. linc01614 was notably upregulated in PC tissues and cell lines and was associated with the poor disease-free survival of patients with PC according to the analysis of The Cancer Genome Atlas-derived datasets. Functionally, linc01614 knockdown suppressed PC cell proliferation, migration and invasion *in vitro*, and inhibited tumor proliferation *in vitro* and *in vivo*. Mechanistically, linc01614 overexpression stabilized the level of β-catenin protein to hyperactivate the WNT/β-catenin signaling pathway in PC cells. Further analyses revealed that linc01614 bound to GSK-3β and perturbed the interaction between GSK-3β and AXIN1, thereby preventing the formation of the β-catenin degradation complex and reducing the degradation of β-catenin. In summary, the present findings reveal that linc01614 may function as an oncogene and promote the progression of PC and may thus be considered as a potential therapeutic target in the future.

*Correspondence to:* Dr Zhi-Gang Tang, Department of Pancreatic Surgery, Renmin Hospital of Wuhan University, 238 Jiefang Road, Wuhan, Hubei 430060, P.R. China
E-mail: rm002251@whu.edu.cn

*Contributed equally

*Key words:* pancreatic cancer, linc01614, WNT/β-catenin signaling pathway, GSK-3β

## Introduction

Pancreatic cancer (PC) is an extremely aggressive malignant tumor and the fourth leading cause of cancer-related mortality in the USA, accounting for an estimated 57,600 new cases and 47,050 related deaths each year (1). It has been also predicted to become the second leading cause of cancer-related mortality in the ensuing 20-30 years (2). Moreover, the incidence of PC tends to increase further as the population ages (2). Due to its aggressive nature and early metastatic behavior, the majority of patients with PC exhibit a poor prognosis and resistance to most treatment strategies, including chemotherapy, radiotherapy and immunotherapy. Several studies have demonstrated a genomic, epigenetic and metabolic remodeling that occurs during the onset and progression of PC, leading to the complexities of tumor tissue, stromal tissue, and the tumor-related immune system and their crosstalk (3,4). Thus, an improved understanding of the underlying mechanisms regulating PC tumorigenesis and tumor development would contribute to the prevention of and therapeutic improvements for PC.

Long non-coding RNAs (lncRNAs) are a novel and abundant type of transcripts, >200 nucleotides in length, although with a limited protein-coding potential (5). lncRNAs are novel regulators of oncogenesis, exerting oncogenic and tumor-suppressive effects in various tumors (6-9). Acting as signals, decoys, guides, and scaffolds, lncRNAs have been reported to form complex networks, in order to modulate multiple cancer phenotypes. Furthermore, they may regulate target gene expression and interact with various cellular components, including DNAs, RNAs and proteins (10,11). For instance, Gandhi *et al* (12) demonstrated that lncRNA lincNMR regulated nucleotide metabolism through its binding to YBX1 protein and affecting the key dNTP synthesizing enzymes RRM2, TYMS and TK1. Additionally, the down-regulation of lincNMR was found to decreased dNTP levels and cell proliferation, and induce senescence in multiple cancer types (12). In another study, Hu *et al* (8) revealed that the lncRNA XLOC-000647 downregulated the expression of its adjacent genes associated with the NLRP3 inflammasome

in *cis*. High XLOC-000647 expression levels may markedly attenuate PC cell proliferation. With advancements being made in transcriptome-sequencing and functional genomics analysis, a number of previously unsuspected lncRNAs have been identified in PC, providing new perspectives towards the further elucidation of PC pathogenesis (13). However, the biological functions of the majority of lncRNAs remain largely unknown.

Hence, the present study was designed to examine the expression patterns and functions of lncRNAs in PC. Bioinformatics analysis was first performed on publicly available genomic databases to recognize lncRNAs aberrantly expressed in PC. It was identified that linc01614 was upregulated in PC and thus it was subjected to further investigations. Functionally, linc01614 significantly promoted the progression of PC *in vitro* and *in vivo*. Moreover, RNA pull-down and co-immunoprecipitation (Co-IP) assays indicated that linc01614 combined with GSK-3β to perturb the interaction between GSK-3β and AXIN1, activated the WNT/β-catenin signaling pathway and consequently enhanced β-catenin protein expression levels. Thus, the results of the present study revealed that linc01614 may be used as a candidate therapeutic target for PC.

## Materials and methods

*Patients and samples*. In total, 20 formalin-fixed and paraffin-embedded PC and normal cancer-adjacent pancreatic tissues were retrieved between September, 2020 to September, 2021 from the Pathological Department of Renmin Hospital of Wuhan University for fluorescent *in situ* hybridization (FISH) analysis. The median age of the patients was 66.5 years (range, 49-79 years). The clinicopathological parameters are summarized in Table SI. The present study was approved by the Ethics Committee and the Human Research Review Committee of Renmin Hospital of Wuhan University (approval no. WDRY2021-K188), and written informed consent was obtained from all subjects.

*Culture and transfection of cell lines*. The PC cell lines, Panc-1 (cat. no. CRL-1469), SW1990 (cat. no. CRL-2172), BXPC-3 (cat. no. CRL-1687) and MIA-PaCa (cat. no. CRL-1420), were purchased from the American Type Culture Collection (ATCC). HPDE cells were obtained from Hunan Fenghui Biotechnology Co., Ltd. (cat. no. CL0317). All the cells were cultured according to the manufacturer's instructions. The cell lines were authenticated by DNA fingerprinting and checked for mycoplasma contamination (data not shown). The cells were cultured in Dulbecco's modified Eagle's medium (DMEM; HyClone, Cytiva) supplemented with 10% fetal bovine serum (Tianhang Biotechnology Co., Ltd.). All cell lines were cultured in a 5% $CO_2$ and 95% humidity incubator at 37˚C.

Antisense oligonucleotides (ASOs) targeting linc01614 and control ASO were obtained from RiboBio, Inc. Transfection of ASOs was conducted using Neofect™ transfection Reagent (Neofect Biotech Co., Ltd.) with the final ASO concentration of 70 nM. The ASO sequences are included in Table SII. To overexpress linc01614, the cDNA was designed, synthesized and then cloned into GV658 vector (Genchem, Inc.). 2 $\mu$g linc01614 plasmid, and corresponding empty vector were transfected into HPDE cells using Neofect™ transfection Reagent (Neofect Biotech Co., Ltd.). The cells were then cultured in a 5% $CO_2$-humidified incubator at 37˚C. After 48 h, the cells were employed to perform subsequent experimentation.

*RNA isolation and reverse transcription-quantitative polymerase chain reaction (RT-qPCR)*. Total RNA was extracted from the cultured cells using TRIzol reagent (Takara Bio, Inc.). All lncRNAs and mRNAs were reverse transcribed with random and oligo dT primers using the reverse transcription kit (cat. no. RR037A; Takara Bio, Inc.). The reaction conditions were as follows: 37˚C for 15 min and 85˚C for 5 sec. Subsequently, qPCR was conducted using the TB green Premix Ex Taq™ II (cat. no. RR820A; Takara Bio, Inc.) on a Bio-Rad 7500 PCR system (Bio-Rad Laboratories, Inc.). The reaction conditions were as follows: Initial denaturation at 95˚C for 30 sec, followed by 40 cycles of amplification at 95˚C for 5 sec and 60˚C for 30 sec, and melt curve analysis at 95˚C for 10 sec and 65˚C for 5 sec. GAPDH or U6 were used as reference genes. The qPCR results were calculated using the $2^{\Delta\Delta Cq}$ method (14). The primers used are presented in Table SIII. The experiments were performed in triplicate.

*RNA FISH*. A fluorescent *in situ* hybridization kit (RiboBio, Inc.) was used to conduct the FISH assay. Briefly, the Panc-1 and SW1990 cells were fixed using 4% paraformaldehyde (Biosharp, Inc.) and washed three times using phosphate-buffered saline (PBS). The cells were then incubated with Cy3-labeled linc01614 RNA probes (RiboBio, Inc.) in a hybridization buffer overnight at 37˚C. The nucleus of cells was stained with 4',6-diamidino-2-phenylindole (DAPI) (RiboBio, Inc.) for 10 min at room temperature. The stainings were observed using a confocal microscope (Olympus FV1200; Olympus Corporation).

For PC tissues, lncRNA FISH on paraffin tissue sections with linc01614 probes was also performed using the same hybridization kit (RiboBio, Inc.). The sections were deparaffinized and rehydrated using xylene and a graded alcohol solution series. Following treatment with protease K (Biosharp, Inc.), the sections were incubated with Cy3-labeled linc01614 probes in hybridization buffer at 37˚C overnight. Cell nuclei were stained with DAPI. Images were acquired with the use of an Olympus fluorescence microscope (Olympus IX71, Olympus Corporation).

*Subcellular fractionation*. Cytoplasmic and nuclear fractions of Panc-1 and SW1990 cells were isolated using the PARIS Kit (Invitrogen; Thermo Fischer Scientific, Inc.). The expression levels of mRNAs and proteins isolated from cytoplasmic and nuclear fractions were measured. GAPDH was used as the control for cytoplasmic expression in RT-qPCR and western blot assays. U6 and LaminB were used as the controls for nuclear expression in RT-qPCR and western blot analysis, respectively.

*CCK-8 and EdU assay*. Cell proliferation was assessed using a Cell Counting Kit-8 (CCK-8; MCE, Inc.) and EdU Cell Proliferation Kit (Epizyme, Inc.). In the CCK-8 assay, Panc-1 and SW1990 cells were seeded on 96-well plates at a density

of 2,000 cells/well, and were then treated with 10 $\mu$l CCK-8 solution from day 1 to 5. Following incubation for 2 h at 37˚C, the absorbance was determined at 450 nm using a microplate reader (HBS-1096A, DeTie Laboratory Equipment Co., Ltd.). For the EdU assay, transfected cells were seeded on 6-well plates, and 10 $\mu$M EdU were added to the well. Following incubation for 2 h at 37˚C, all cells were fixed with 4% paraformaldehyde (Biosharp, Inc.), washed three times with PBS containing 3% BSA, penetrated with PBS containing 0.3% Triton X-100, washed three times with PBS containing 3% BSA, and 500 $\mu$l Click Additive Solution (Epizyme, Inc.) was then added for 30 min at room temperature in the dark. Finally, the nucleus of the cells was stained with Hoechst 33342 (Epizyme, Inc.) for 10 min at room temperature in the dark. Images were acquired using an Olympus fluorescence microscope (Olympus IX71, Olympus Corporation).

*Colony formation assay*. Panc-1 and SW1990 cells were seeded in 6-well plates at a concentration of 1,000 cells per well and cultured in DMEM medium supplemented with 10% fetal bovine serum. Following a 2-week incubation at 37˚C, all cells were washed twice with PBS (Cienry, Inc.), fixed with 4% paraformaldehyde (Biosharp, Inc.), and stained with 0.1% crystal violet (Biosharp, Inc.) for 30 min. Finally, the colonies were imaged using a camera (Redmi 10x4G, Xiaomi Corporation) and counted using Image J software (National Institutes of Health).

*Transwell assay*. Cell migration and invasion were assessed using the Transwell assay. The upper chambers of the Transwells (Corning, Inc.) were coated with 1:8 diluted Matrigel (BD Biosciences) or without Matrigel for invasion and migration, respectively. A total of $5x10^4$ cells (Panc-1 and SW1990) was plated in the upper chambers with 100 $\mu$l serum-free medium, while the lower chambers were plated with 600 $\mu$l DMEM medium (HyClone, Cytiva), containing 15% fetal bovine serum (Tianhang Biotechnology Co., Ltd.). Following incubation for 24-48 h at 37˚C, the cells on the upper surface were cleared using a cotton swab, and the cells on the lower surface were fixed with 4% paraformaldehyde, stained with 0.1% crystal violet (Biosharp, Inc.) for 30 min. The results were examined and photographed using an Olympus microscope (Olympus IX71, Olympus Corporation).

*Wound healing assay*. Panc-1 and SW1990 cells were seeded in 6-well plates and cultured in DMEM supplemented with 1.5% fetal bovine serum. When the cells reached 90% confluency, the cell wound was then generated utilizing a 10 $\mu$l pipette tip. The percentage of wound closure [(original width-width after cell migration)/original width] was examined and photographed at 0 and 48 h (Olympus IX71, Olympus Corporation).

*Flow cytometry*. For the analysis of the cell cycle, Panc-1 and SW1990 cells were harvested, washed with PBS, stained with binding buffer containing 1 ml DNA staining solution and 10 $\mu$l permeabilization solution, and incubated at room temperature for 30 min in the dark according to the manufacturer's instructions (MultiSciences Biotech, Co., Ltd.). For the analysis of cell apoptosis, cells were collected, washed in PBS, and resuspended in a 500 $\mu$l mixture of 5 $\mu$l Annexin V-FITC (Annexin V-PE) and 10 $\mu$l propidium iodide (7-AAD; MultiSciences Biotech, Co., Ltd.). Modfit (Verity Software House, Inc.) and FlowJo V10 (TreeStar, Inc.) software were employed to analyze the cell cycle and apoptosis data, respectively.

*Western blot analysis*. Total protein was extracted from Panc-1 and SW1990 cells using RIPA lysis buffer (Beyotime Institute of Biotechnology). Protein concentrations were determined using the BCA Protein Assay kit (Beyotime Institute of Biotechnology). Subsequently, 20 $\mu$g proteins from each sample were loaded, separated by 10% SDS-PAGE gels, and then transferred onto a polyvinylidene difluoride membrane (MilliporeSigma). After being blocked with Protein Free Rapid Blocking Buffer (Epizyme, Inc.) for 30-60 min at room temperature, the membrane was incubated with the following primary antibodies: Cyclin D1 (cat. no. WL01345a; 1:500), CDK2 (cat. no. WL01543; 1:1,500), E-cadherin (cat. no. WL01482; 1:1,000), N-cadherin (cat. no. WL01047; 1:1,000), Snail (cat. no. WL01863; 1:1,000), twist-related protein 1 (Twist1; cat. no. WL00997; 1:500), β-catenin (cat. no. WL00962; 1:1,000), adenomatous polyposis coli (APC; cat. no. WL02422; 1:500) and LaminB (cat. no. WL01775; 1:1,000) (all from WanleiBio, Co., Ltd.); GSK-3β (cat. no. 22104-1-AP; 1:2,000) and AXIN1 (cat. no. 16541-1-AP; 1:500) from ProteinTech Group, Inc.; active β-catenin (cat. no. 8814, 1:1,000) from Cell Signaling Technology, Inc.; Vimentin (cat. no. GB111308; 1:1,000) and β-actin (cat. no. GB11001; 1:1,000) from Servicebio Technology Co., Ltd.; and GAPDH (cat. no. ABPR001; 1:2,000) from Goodhere, Inc. (https://www.goodhere.com/kysj/) at 4˚C overnight. On the second day, the membrane was washed three times using Tris-buffered saline with 0.1% Tween (TBST) and incubated with a goat anti-rabbit secondary antibody (cat. no. G1213; 1:3,000; Servicebio Technology Co., Ltd.;) for 1 h at room temperature. Finally, the signals of the immunoreactive protein bands were detected with a Biosharp ECL detection kit (Biosharp, Inc.). The WNT/β-catenin activator LiCl (Sigma-Aldrich; Merck KGaA) was used to further investigate the association between linc01614 and WNT/β-catenin pathway in PC cells. PC cells were transfected with antisense oligonucleotide (ASO)-NC or ASO-1 for 24 h and then treated with 20 mM LiCl for 24 h. Data were analyzed using ImageJ software (v. 1.46; National Institutes of Health).

*Xenograft tumors*. A total of 10 male BALB/c-nu mice (aged 4 weeks) were purchased from the Hunan SJA Laboratory Animal Center. All mice were housed under specific-pathogen-free conditions (temperature, 25˚C; humidity, 50%; light/dark cycle, 12/12 h cycle), with food and water *ad libitum*. Animal health and behavior were monitored every day. Panc-1 tumor cells ($1x10^7$) were suspended in 200 $\mu$l of sterile PBS and subcutaneously injected into the right flanks of mice. After the tumors were palpable, xenograft mice were grouped randomly as negative control (n=5) and ASO-1 group (n=5). Then, 5 nM ASO-NC or ASO-1 were injected intratumorally every 3 days for 4 times in total. The tumor size was measured using a caliper every week. Tumor volume was estimated as (length x $width^2$)/2. After 3 weeks, the mice were euthanized using 1% pentobarbital sodium (50 mg/kg, intraperitoneal) followed by cervical dislocation. Death was verified

by the cessation of respiration and heartbeat, and the absence of reflexes. Subsequently, the tumors were isolated and maintained in liquid nitrogen for further analysis. All experiments were conducted according to the relevant guidelines and regulations and following the approval of the Institutional Animal Care Committee of Renmin Hospital of Wuhan University (approval no. WDRM20210606). The humane endpoints of the experiment were as follows: i) A significant increase in tumor burden (≥10% body weight); ii) weight loss ≥20% body weight; iii) occurrence of ulceration or infection at the site of tumor and surrounding tissue; iv) no movement for >24 h; v) no eating or drinking. In this experiment, no animal reached the humane endpoints and none of the mice were found dead.

*Immunohistochemistry*. Paraffin-embedded tissue sections were deparaffinized and rehydrated using xylene and a graded alcohol solution series as follows: Xylene I for 30 min, xylene II for 10 min, 100% ethanol I for 10 min, 100% ethanol II for 3 min, 90% ethanol for 3 min, 70% ethanol for 3 min and $H_2O$ for 3 min. Subsequently, antigen retrieval was performed using microwave heating in 10 mM citrate buffer (Servicebio Technology Co., Ltd.). Endogenous peroxidase was blocked with 3% $H_2O_2$. Subsequently, the sections were incubated with primary antibodies specific for proliferating cell nuclear antigen (PCNA; ProteinTech Group, Inc.; cat. no. 10205-2-AP; 1:200), Ki67 (ProteinTech Group, Inc.; cat. no. 27309-1-AP; 1:200) and β-catenin (Wanleibio, Co., Ltd.; cat.no. WL00962; 1:50) at 4˚C overnight. On the second day, the slides were incubated with a goat anti-rabbit secondary antibody (1:200; cat. no. G1213; Servicebio Technology Co., Ltd.) for 30 min at room temperature. The results were assessed independently by two pathologists, and photographed using an Olympus microscope (Olympus BX51 TRF, Olympus Corporation). The staining intensity was scored from 0 to 3, and the proportion of staining ranged from 0 to 4. The immunoreactive score was obtained by multiplying the proportion and intensity scores. A total score higher than 4 was considered a high expression (15). ImageJ software (v. 1.46; National Institutes of Health) was used to analyze the relative protein expression.

*TOP/FOP flash assay*. In brief, the cells were added to a 24-well plate and transfected with ASO-NC or ASO-linc01614 in the presence of TOP Flash or FOP Flash plasmid and *Renilla* luciferase reporter plasmid (Beyotime Institute of Biotechnology) using a Neofect™ transfection Reagent (Neofect Biotech Co., Ltd.). Following 48 h of incubation at 37˚C, luciferase intensity was detected utilizing a Dual-Luciferase Reporter Assay System (GloMax™; Promega Corporation). Finally, the relative ratio of TOP flash value/FOP flash value was calculated and used as an indicator of the activation of the WNT/β-catenin signaling pathway.

*RNA pull-down assay*. Biotin-labeled lncRNAs were transcribed and purified using the T7 Biotin Labeling Transcription kit (Invitrogen; Thermo Fischer Scientific, Inc.). Subsequently, biotinylated RNA was mixed with the cell lysates for 4 h and incubated with streptavidin agarose magnetic beads (cat. no. G1213; Thermo Fisher Scientific, Inc.) for 1 h at room temperature. Finally, the purified RNA-proteins complexes were washed, resolved and subjected to mass spectrometry or western blot analysis. For mass spectrometry, the gel piece was washed, in-gel digested, and the peptides were extracted. The peptides were then selected using an autosampler and transferred into a C18 analytical column for separation. For DDA mode analysis, each scan cycle consisted of one full-scan mass spectrum followed by 40 MS/MS events. Former target ion exclusion was set for 12 sec. LC-MS/MS analysis was performed on a quadrupole-TOF LC-MS/MS mass spectrometer (TripleTOF 5600 plus, SCIEX) coupled with an Ekspert 400 MicroLC system. Raw data were analyzed using MaxQuant (V1.6.6) using the Andromeda database search algorithm.

*RNA immunoprecipitation (RIP) assay*. RIP assay was conducted using an RNA Immunoprecipitation kit (Geneseed Biotech Co., Ltd.). Panc-1 and SW1990 cells were harvested and lysed using RIP lysis buffer. Subsequently, the whole lysates were incubated with magnetic beads conjugated to 5 $\mu$g anti-GSK-3β antibodies (cat. no. 22104-1-AP; ProteinTech Group, Inc.), or IgG (GB111738; Servicebio Technology Co., Ltd.) at 4˚C overnight. The immunoprecipitated RNAs were isolated and subjected to RT-qPCR analysis.

*Co-IP assay*. Co-IP assay was conducted using an Immunoprecipitation kit (cat. no. ab206996; Abcam Co., Ltd.). PC cells were harvested and lysed using immunoprecipitation lysis buffer. Subsequently, cell extracts were incubated with the 2 $\mu$g indicated antibodies: GSK-3β (cat. no. 22104-1-AP; ProteinTech Group, Inc.) and AXIN1 (cat. no. 2087S; Cell Signaling Technology, Inc.) at 4˚C overnight, followed by incubation with Protein A/G magnetic beads for 4 h. Finally, the immunoprecipitates were collected and examined by western blot analysis.

*Bioinformatics and statistical analysis*. The expression and survival analyses for lncRNAs in PC were obtained from The Cancer Genome Atlas (TCGA; https://www.cancer. gov/about-nci/organization/ccg/research/structural-genomics/tcga) and Genotype-Tissue Expression project (GTEx; https://www.genome.gov/Funded-Programs-Projects/Genotype-Tissue-Expression-Project). TGCA and GTEx datasets were analyzed using the R software. The t-distributed stochastic neighbor embedding (t-SNE) and pan-cancer analysis were conducted using an online tool Sangerbox (http://sangerbox.com). Gene set enrichment analysis was performed using the GSEA software (v.4.0; Broad Institute, Inc.). The RPISeq (http://pridb.gdcb.iastate.edu/RPISeq) and catRAPID (http://service.tartaglialab.com) databases were employed to predict the RNA-Protein interaction. Experiments were performed in triplicate. The results were analyzed using the SPSS 17.0 (SPSS, Inc.) or GraphPad Prism 8.0 (GraphPad Software, Inc.) software and represented as percentages or mean ± standard deviation. The Kaplan-Meier method was employed to evaluate the overall survival (OS) and disease-free survival (DFS). The two-tailed unpaired Student's t-test was employed to analyze the means of two groups. One-way ANOVA was employed to evaluate the differences among multiple groups. As a post hoc test following ANOVA, Dunnett's multiple comparisons test was used for comparisons with only the control group and

Tukey's multiple comparisons test was used for comparisons among multiple pairs of groups. The association of linc01614 expression with the clinical parameters of patients with PC was assessed using the Chi-squared test ($\chi^2$). $P<0.05$ was considered to indicate a statistically significant difference.

## Results

*Identification of linc01614 as a PC-related lncRNA*. To explore whether lncRNAs may be potentially related to PC, a genomic analysis of gene expression data obtained from the TCGA and GTEx database was conducted and 6,072 lncRNAs were identified. Upon setting the thresholds to a fold change >2 and a false discovery rate (FDR) <0.01, 207 lncRNAs were found to be dysregulated in PC, of which 104 were upregulated and 103 downregulated (Fig. 1A and B, Table SIV). Hierarchical clustering and t-SNE analysis revealed the notable differentiation of these lncRNAs between the PC and non-cancerous pancreatic tissues (Fig. 1C and D). Subsequently, in order to determine to what extent these lncRNAs have been previously studied in tumors, articles published in PubMed up to January 8, 2022 were systematically retrieved. It was observed that a number of lncRNAs, including UCA1, linc00460, CASC9, MEG3, NEAT1 and ROCR, have already been studied in cancer research (Fig. 1E).

linc01614 emerged as one of the prominently differentially expressed lncRNAs in PC, as compared to non-cancerous pancreatic tissues, with a log FC of 5.8 and FDR of 2.20E-52. As the authors wished to mainly focus on oncogenic factors, the present study mainly focused on upregulated lncRNAs, since oncogenic lncRNAs are preferable therapeutic targets and diagnostic or prognostic biomarkers. The expression of linc01614 across different tumor types was evaluated. As demonstrated in Fig. 1F, PC had the second highest linc01614 expression among various tumor types. Subsequently, the PubMed database was investigated and it was observed that the function of linc01614 as a potential biomarker and oncogene in gastric cancer (16), breast cancer (17), lung cancer (18,19), osteosarcoma (20) and esophageal squamous cell carcinoma (21) has already been studied. However, the biological roles and mechanisms of action of linc01614 in PC remain relatively unknown. Additionally, bioinformatics analysis of online databases predicted that linc01614 may perform a regulatory function by interacting with more RNAs and proteins (Table SV, and Fig. 7B and C). linc01614 is also closely associated with several signaling pathways, including WNT/β-catenin, TGF-β, and focal adhesion kinase signaling, thus suggesting that linc01614 is worthy of investigation in PC (Fig. 6A). Thus, it was decided to evaluate the biological functions and mechanisms of linc01614 in PC with further experiments.

*linc01614 is upregulated in PC and is associated with poor DFS*. The expression pattern of linc01614 was first investigated using the publicly available RNA-sequencing data from the GTEx and TCGA databases. The level of linc01614 was higher in PC tissues than non-tumor tissues (Fig. 2A). Moreover, linc01614 expression was negatively associated with the DFS rather than OS (Fig. 2B and C). The association between linc01614 expression and routine clinicopathological parameters was also evaluated, based on TCGA database. The results did not reveal any significant association between linc01614 level and the routine clinicopathological parameters in patients with PC, including age, sex, tumor size, tumor location, histological grade, tumor, node, and metastasis (TNM) stage and the number of positive lymph nodes. The results are summarized in Table SVI. The expression of linc01614 was then analyzed in a cohort of 20 cases of formalin-fixed paraffin-embedded PC tissues and adjacent non-cancerous tissues using RNA FISH analysis. An increased level of linc01614 in PC tissues was observed (Fig. 2D).

Subsequently, the linc01614 levels were investigated in various PC cell lines (Panc-1, SW1990, BxPC-3 and Mia-PaCa) using RT-qPCR. linc01614 expression in PC cell lines was also significantly elevated in comparison with the human pancreatic duct epithelium immortalized cells (HPDE; Fig. 2E). As the localization of lncRNA significantly affects its function, the present study then aimed to identify the localization of linc01614 in Panc-1 and SW1990 cells, using the RNA FISH assay and subcellular fractionation. linc01614 was located in both the cytoplasm and nucleus, although its abundance was slightly higher in the cytoplasm than nucleus (Fig. 2F and G).

*linc01614 promotes the proliferation of PC cells in vitro*. To determine the biological function of linc01614 in PC cells, two independent ASOs against human linc01614 (ASO-1 and ASO-2) were applied to knockdown linc01614 in Panc-1 and SW1990 cells, and the knockdown efficiency was examined using RT-qPCR (Fig. 3A). The results of CCK-8 assay revealed that the knockdown of linc01614 suppressed the proliferation of PC cells (Fig. 3B). This finding was further verified by the EdU (Fig. 3C) and colony formation (Fig. 3D) assays. Cell cycle distribution in the PC cells was also detected using flow cytometry. Notably, the results revealed an increase in the number of PC cells in the G1/G0 phase and a decrease in the number of PC cells in the S phase following linc01614 knockdown compared with the control (Fig. 3E). To further verify the flow cytometry data, western blot analysis was performed to detect the G0/G1 phase regulating proteins cyclin D1 and CDK2. linc01614 knockdown decreased the expression of cyclin D1 and CDK2 in Panc-1 and SW1990 cells in comparison with the control group (Fig. 3F). Furthermore, flow cytometry results revealed no significant difference in apoptosis between linc01614 knockdown and control groups in both the Panc-1 and SW1990 cells (Fig. S1).

Additionally, linc01614 overexpression was also induced in HPDE cells by plasmid transfection. EdU and flow cytometry assays were performed to investigate the effects of linc01614 on cell proliferation and apoptosis in HPDE, respectively. The results revealed that linc01614 overexpression promoted HPDE cell proliferation, whereas no significant differences in apoptosis were observed between the linc01614 upregulated and control HPDE cells (Fig. S2).

*linc01614 promotes the migration and invasion of PC cells in vitro*. The effects of linc01614 on the migration and invasion of PC cells were explored using wound healing and Transwell assays, respectively. linc01614 knockdown markedly decreased cell migration and invasion as compared to the control (Fig. 4A and B).

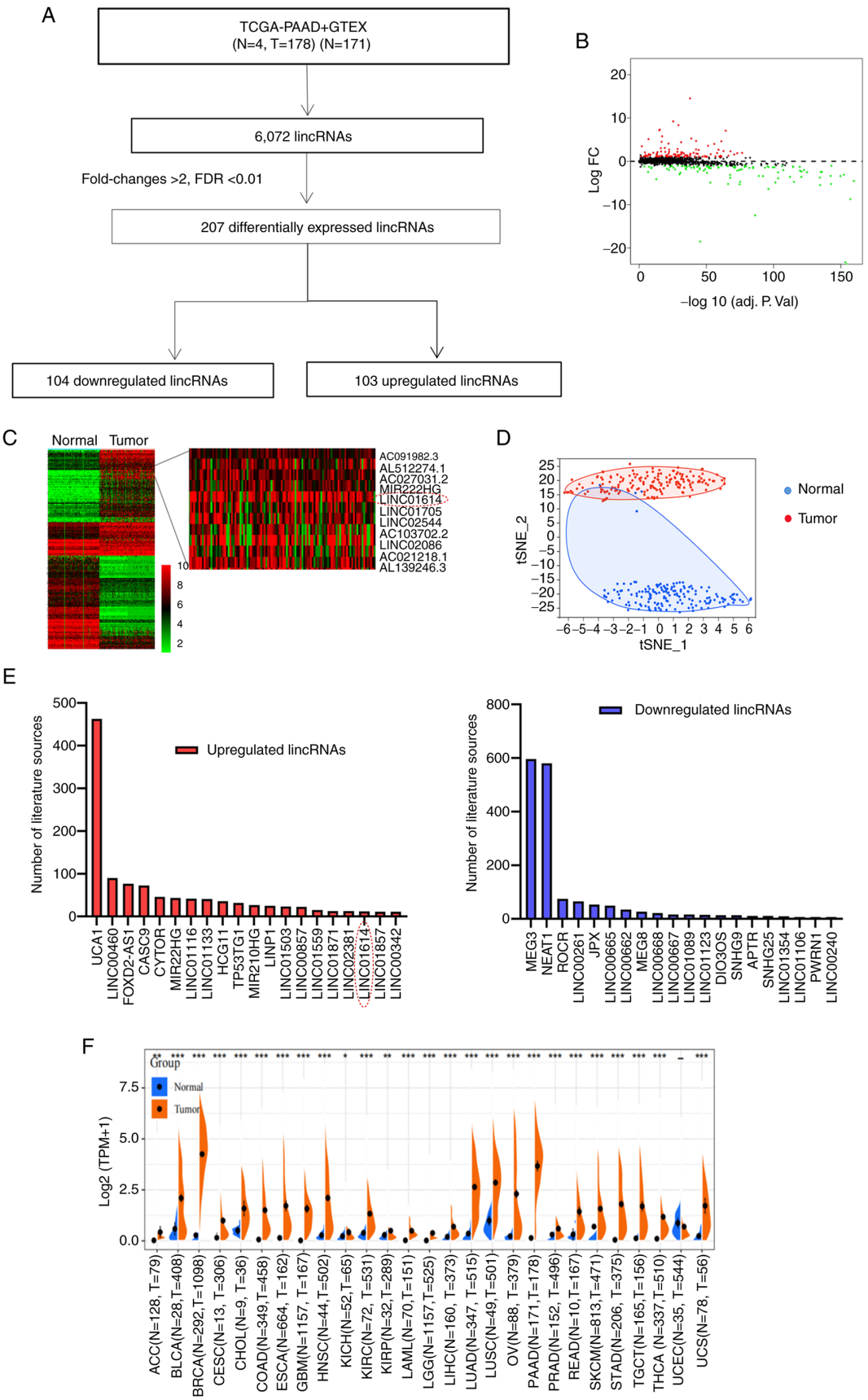


Figure 1. Identification of linc01614 as a PC-related lncRNA. (A) Study scheme on screening PC-related lncRNAs from TCGA and GTEx database (N, normal; T, tumor). (B) Volcano plot of lncRNA expression changes between PC and normal samples. (C and D) Cluster heatmap and t-SNE analysis illustrating the distribution of differentially expressed lncRNAs between PC and normal samples. The red and green dots represent upregulated and downregulated lncRNAs, respectively. (E) Number of studies on the top 20 most published lncRNAs concerning pan-cancer analyses. The left panel corresponds to upregulated lncRNAs and the right panel to downregulated lncRNAs. (F) Expression of linc01614 according to pan-cancer analyses of the TCGA and GTEx databases. PC, pancreatic cancer; lncRNA, long non-coding RNA; TCGA, The Cancer Genome Atlas; GTEx, Genotype-Tissue Expression project; t-SNE, t-distributed stochastic neighbor embedding.

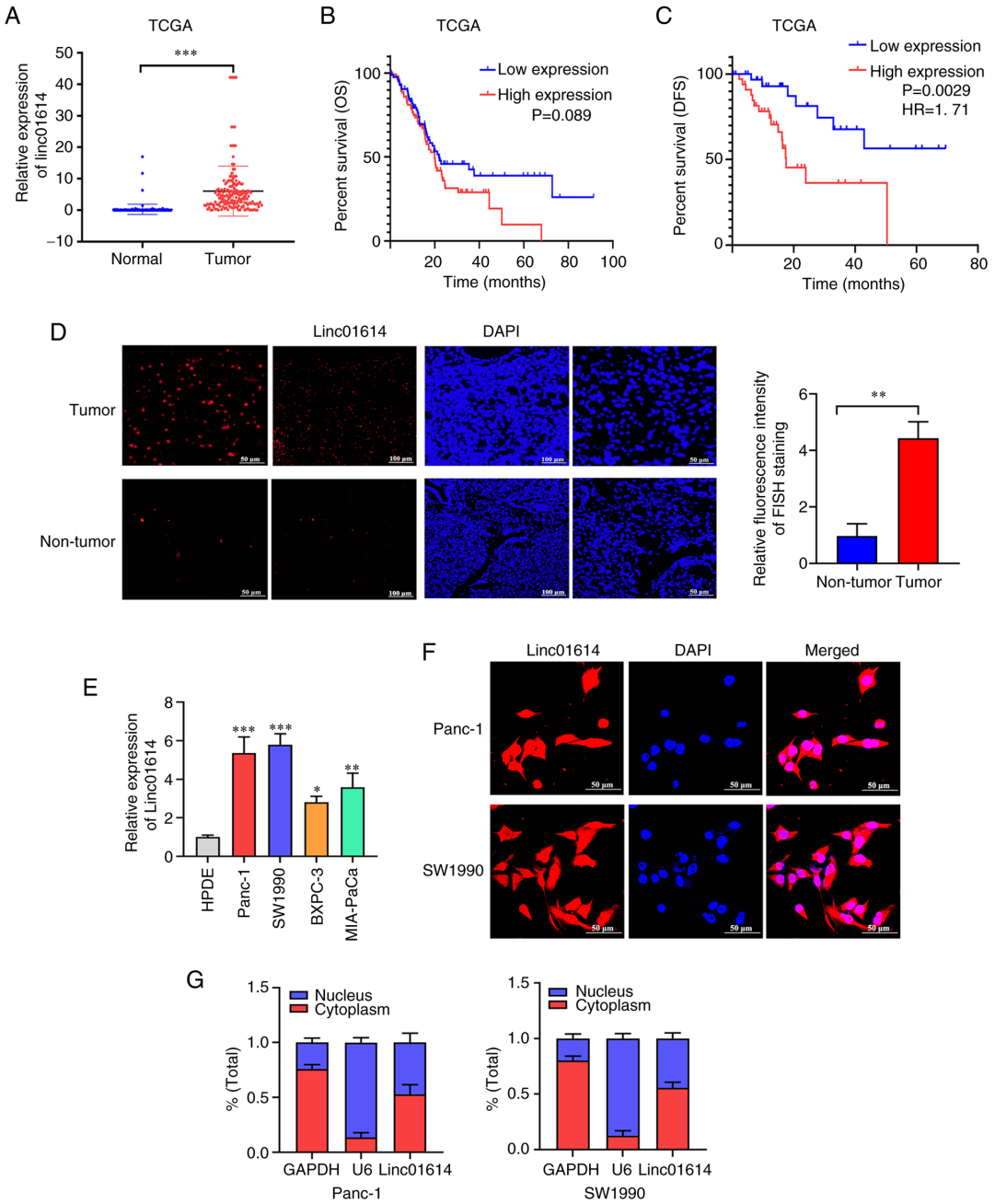


Figure 2. Upregulation of linc01614 in PC. (A) Ectopic expression of linc01614 in PC tissues than in the normal pancreatic tissues from TCGA and GTEx databases (N=171, T=178). (B and C) Data from TCGA, indicating the association of the high expression of linc01614 with poor DFS rather than OS. (D) RNA FISH analysis of the expression of linc01614 in PC and normal pancreatic cancer tissues. Magnification, x200 and x400. (E) Expression of linc01614 in Panc-1, SW1990, BXPC-3 and MIA-PaCa cells vs. HPDE cells. (F) RNA FISH analysis to determine the localization of linc01614. Magnification, x600. (G) Fractionation of PC cells followed by reverse transcription-quantitative PCR, to confirm linc01614 localization. Data are presented as the mean ± SD. $^{*}$P<0.05, $^{**}$P<0.01, $^{***}$P<0.001 vs. the normal tissues or HPDE cells. PC, pancreatic cancer; TCGA, The Cancer Genome Atlas; GTEx, Genotype-Tissue Expression project; DFS, disease-free survival; OS, overall survival; FISH, fluorescent in-situ hybridization; SD, standard deviation.

Accumulating evidence has emerged on the association of invasion and metastasis with the epithelial-mesenchymal transition (EMT) in PC (22-24). Hence, the expression of EMT-related proteins was also evaluated using western blot analysis. The expression of the EMT-related epithelial marker, E-cadherin, markeldy increased, whereas the expression of the mesenchymal markers, N-cadherin, vimentin, Snail and Twist, decreased in the linc01614 knockdown groups (Fig. 4C). These results verified that linc01614 promoted the migration, invasion and EMT of PC cells *in vitro*.

*linc01614 knockdown inhibits tumorigenesis in vivo.* To further validate the results of linc01614 *in vivo*, a xenograft tumor model was established using the Panc-1 cell. It was found that the ASO-1-transfected group generated smaller tumors in nude mice than the control group. The analysis of tumor volume and weight also demonstrated that linc01614 knockdown suppressed tumor growth *in vivo* (Fig. 5A-C). linc01614 expression was also reduced in the xenograft tumors of the ASO-1-transfected group as compared with the control group (Fig. 5D). Immunohistochemical staining revealed that the

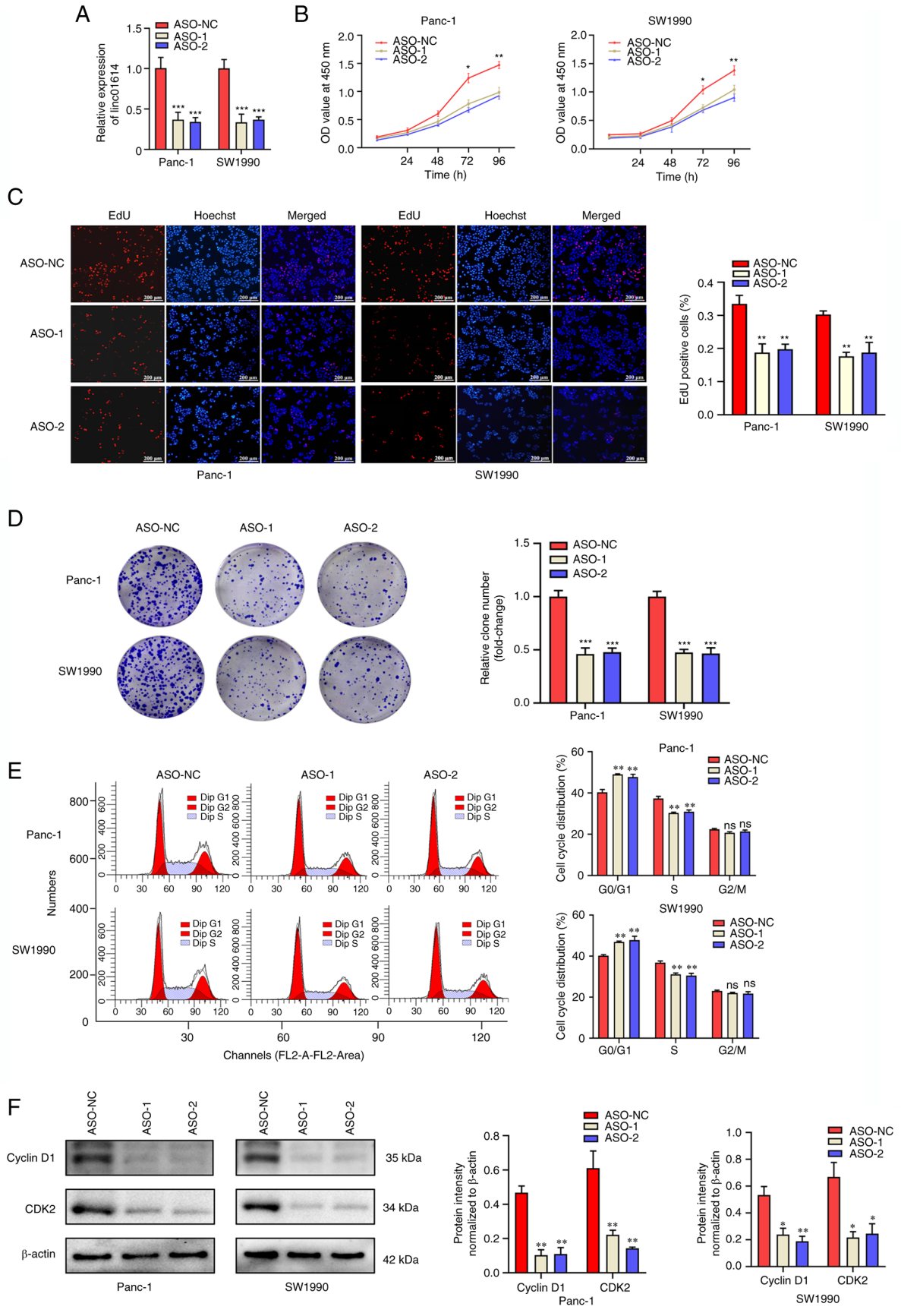


Figure 3. linc01614 promotes PC cell proliferation *in vitro*. (A) Efficacy of linc01614 knockdown in Panc-1 and SW1990 cells by ASOs was detected using reverse transcription-quantitative polymerase chain reaction. (B-D) Effect of linc01614 knockdown on the proliferation of PC as demonstrated by using CCK-8, EdU, and colony formation assays. Magnification, x200. (E) Effect of linc01614 knockdown on cell cycle regulation in PC cells. (F) Expression of cell cycle-associated protein Cyclin D1 and CDK2 in linc01614 knockdown and control group in PC cells. Data are presented as mean ± SD. $^{*}$P<0.05, $^{**}$P<0.01 and $^{***}$P<0.001 vs. the ASO-NC group. PC, pancreatic cancer; ASO, antisense oligonucleotide; CCK, cell counting kit; SD, standard deviation.

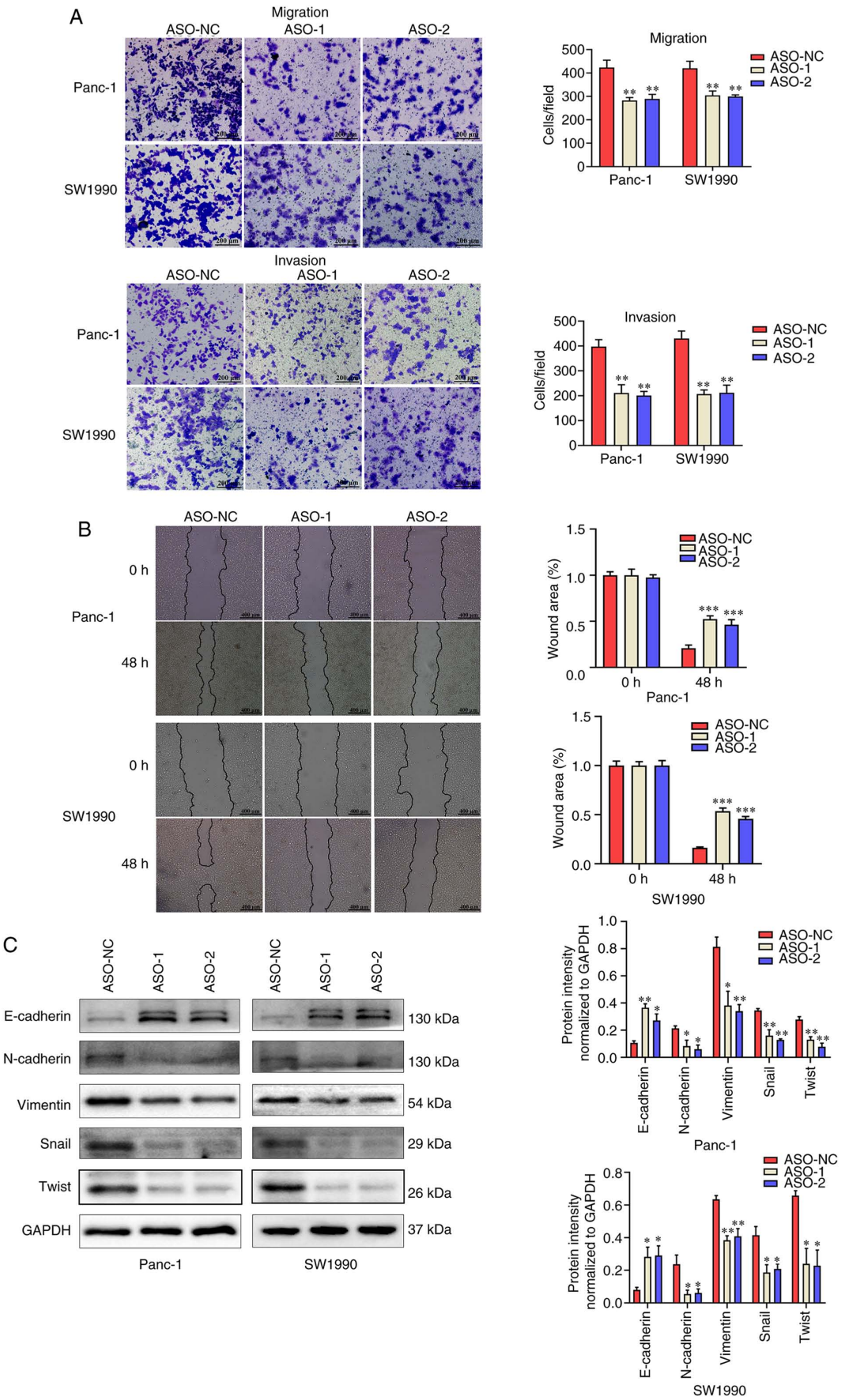


Figure 4. linc01614 facilitates the migration and invasion of PC cells *in vitro*. (A) Transwell assays was used, to assess the migration and invasion abilities of PC cells. Magnification, x100. (B) Wound healing assay, for the examination of Panc-1 and SW1990 cells migration ability upon linc01614 knockdown. Magnification, x40. (C) Western blot analysis was performed for the measurement of EMT-related protein expression in PC cells transfected with ASO-NC and ASO-1. Data are presented as the mean ± SD. $^{*}$P<0.05, $^{**}$P<0.01 and $^{***}$P<0.001 vs. the ASO-NC group. PC, pancreatic cancer; EMT, epithelial-mesenchymal transition; ASO, antisense oligonucleotide; NC, negative control; SD, standard deviation.

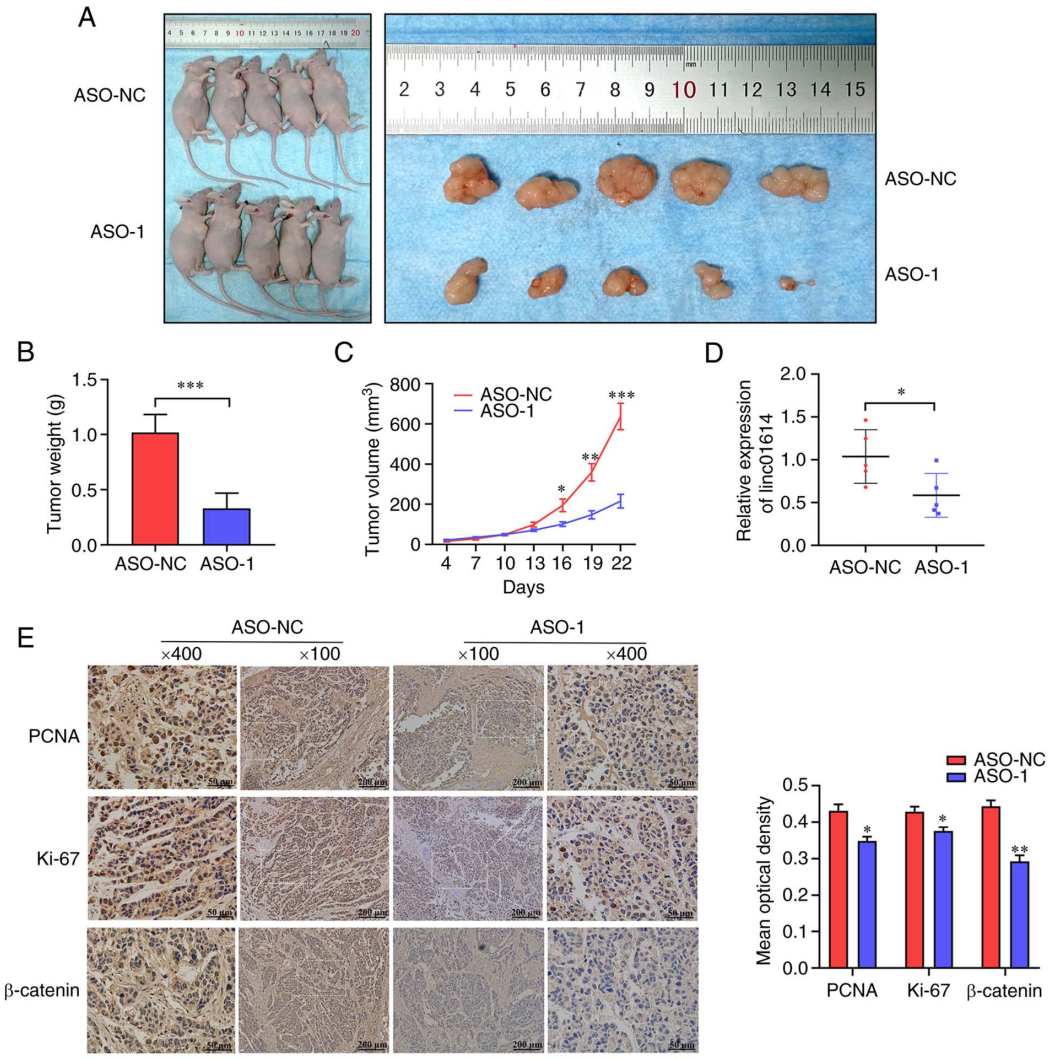


Figure 5. linc01614 knockdown inhibits tumorigenesis *in vivo*. (A) Xenograft tumor formation assays revealed that decreased expression of linc01614 inhibited subcutaneous tumor growth in Panc-1 cells. (B and C) Tumor weight and tumor volume in ASO-NC and ASO-1 groups. (D) Expression of linc01614 in the tumor tissues of the ASO-NC and ASO-1 groups. (E) Representative immunohistochemical staining images demonstrating PCNA, Ki-67 and β-catenin expression in subcutaneous xenograft tumors under different experimental conditions. Magnification, x100 and x 400. Data are presented as the mean ± SD. $^{*}$P<0.05, $^{**}$P<0.01 and $^{***}$P<0.001 vs. the ASO-NC group. ASO, antisense oligonucleotide; NC, negative control; PCNA, proliferating cell nuclear antigen; SD, standard deviation.

tumors derived from the ASO-1 treated group exhibited a lower number of PCNA-, Ki67- and β-catenin-positive cells compared with the control group (Fig. 5E). In brief, linc01614 inhibition by ASO-1 efficiently suppressed tumor growth *in vivo*.

*linc01614 modulates the WNT/β-catenin signaling pathway in PC*. To investigate the potential molecular mechanisms of linc01614 in PC, GSEA analysis was performed. linc01614 was significantly associated with several cancer-related signaling pathways (Fig. 6A), including the WNT/β-catenin signaling pathway, pathways in cancer, pancreatic cancer pathway and TGF-β signaling pathway. The WNT/β-catenin pathway is one of the most crucial signaling pathways in modulating the occurrence of EMT in tumor cells (25-27). In addition, several studies were detected regarding the activation of WNT/β-catenin in PC (27-31). Combined with the EMT results of the present study, it was hypothesized that linc01614 may function as an oncogene partly by modulating the WNT/β-catenin signaling pathway.

Furthermore, the TOP/FOP flash reporter assay was performed to analyze the effects of linc01614 expression on the WNT/β-catenin pathway in PC cells. It was demonstrated that linc01614 knockdown significantly suppressed TOP-Flash reporter activity in Panc-1 and SW1990 cells (Fig. 6B). The expression of several proteins involved in the WNT signaling pathway was then also measured. No significant differences were observed concerning WNT pathway component mRNA levels between the linc01614 knockdown and control groups (Fig. 6C). In the western blot analysis, the expression of β-catenin significantly decreased in the linc01614 knockdown group than in the control group. However, no significant difference in the levels of other proteins, including GSK-3β, APC, and AXIN1, between the linc01614 knockdown and control group were detected (Fig. 6D). Furthermore, the nuclear and cytoplasmic levels of active and total β-catenin were decreased in the linc01614 knockdown in comparison with the control group (Fig. 6E). Hence, it was hypothesized that linc01614 may influence β-catenin expression at the post-transcriptional level.

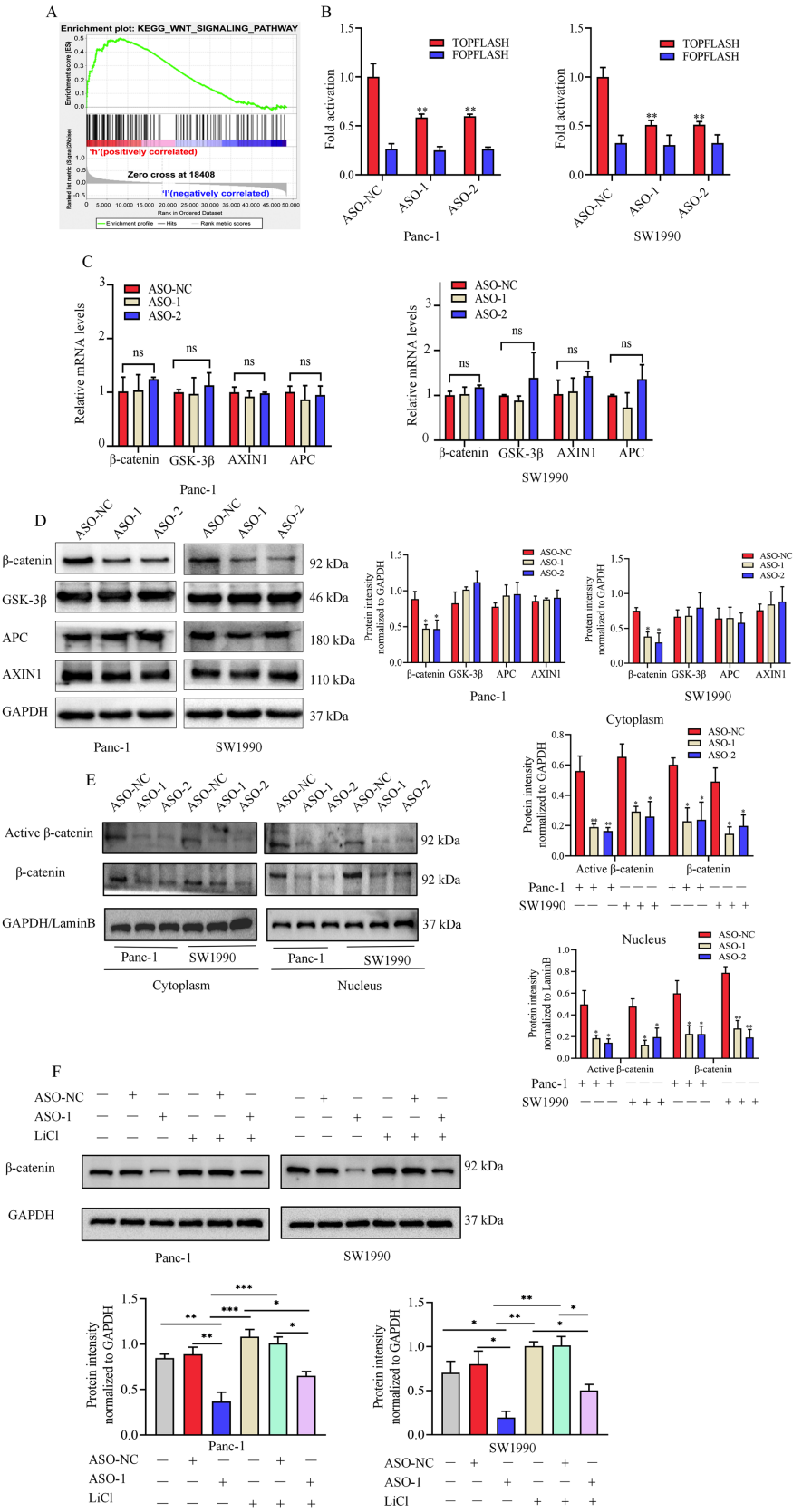


Figure 6. linc01614 perturbs the WNT/β-catenin signaling pathway in PC. (A) GSEA analysis suggesting a positive association between linc01614 and the WNT/β-catenin signaling pathway in PC. (B) TOP/FOP Flash reporter assay, for the examination of the WNT signaling pathway activity in Panc-1 and SW1990 cells following transfection with ASO-NC, ASO-1, or ASO-2. (C and D) mRNA and protein levels of several vital proteins involved in the WNT signaling pathway in ASO-NC-, ASO-1-, or ASO-2-transfected PC cells. (E) Western blot analysis was used to measure the nuclear and cytoplasmic levels of active β-catenin and total β-catenin in PC cells transfected with ASO-NC, ASO-1, or ASO-2. GAPDH and LaminB were used as internal cytoplasmic and nuclear controls, respectively. (F) Western blot analysis of β-catenin in normal PC cells or PC cells treated with ASO-NC, ASO-1, LiCl, ASO-NC + LiCl, and ASO-1 + LiCl. Data are presented as the mean ± SD. (ns, not significant). One-way ANOVA with Tukey's test was employed to compare the expression of β-catenin in each group. $^{*}$P<0.05, $^{**}$P<0.01 and $^{***}$P<0.001. p GSEA, Gene-set enrichment analysis; PC, pancreatic cancer; ASO, antisense oligonucleotide; NC, negative control; SD, standard deviation.

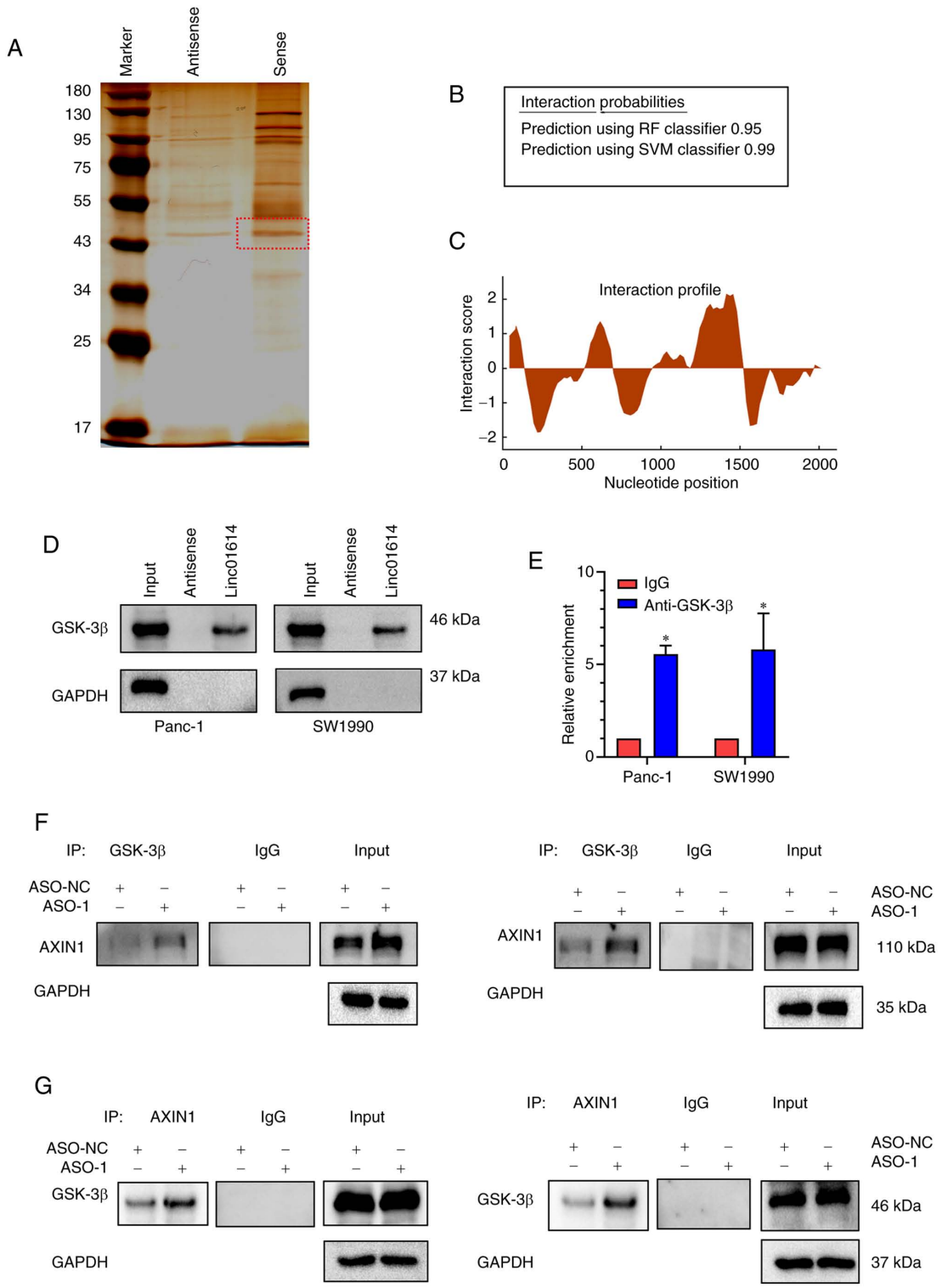


Figure 7. linc01614 combines with GSK-3β to obstruct the interaction between GSK-3β and AXIN1 in Panc-1 and SW1990 cells. (A) RNA pull-down assay followed by silver staining revealed proteins derived from biotinylated linc01614. The red rectangle was analyzed by mass spectrometric analysis and identified as GSK-3β. (B and C) Interaction probabilities and potential binding areas between linc01614 and GSK-3β predicted using the RPISeq and catRAPID databases, respectively. (D) Western blot analysis was used to verify the interaction of GSK-3β with linc01614 using the anti-GSK-3β antibody. (E) RIP assays followed by reverse transcription-quantitative polymerase chain reaction for the validation of linc01614 binding to GSK-3β protein. (F and G) Co-immunoprecipitation assay was applied to determine the effect of linc01614 on the interaction between GSK-3β and AXIN1. The assay revealed that GSK-3β binding to AXIN1 is elevated in linc01614-knocked-down PC cells. Data are presented as the mean ± SD. *P<0.05 vs the IgG group. PC, pancreatic cancer; RIP, RNA immunoprecipitation; SD, standard deviation.

To examine the association between linc01614 and β-catenin in PC cells, WNT signaling was activated in Panc-1 and SW1990 cells using the WNT signaling activator, LiCl. Western blot analysis indicated that LiCl increased the expression of β-catenin and partly offset the effect of linc01614 knockdown in PC cells (Fig. 6F). Taken together, these data

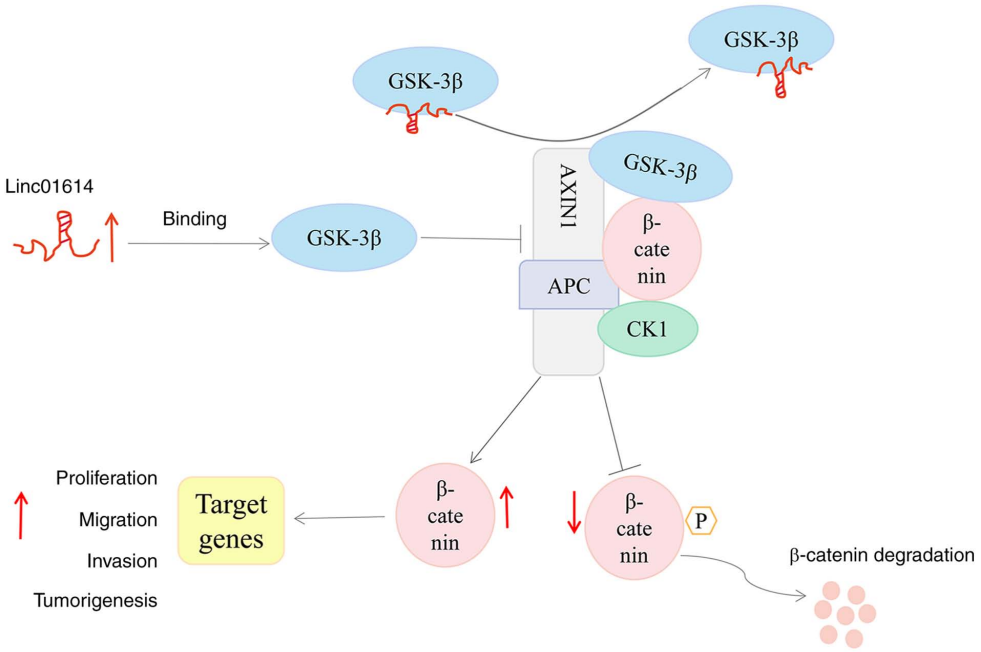


Figure 8. Schematic diagram illustrating tumor promotion mechanism regulated by linc01614 in pancreatic cancer. A high level of linc01614 impedes the interaction between GSK-3β and AXIN1 by binding of the lncRNA to GSK-3β, thereby preventing the formation of the β-catenin 'degradation complex', subsequently reducing the degradation of β-catenin and induces β-catenin accumulation, ultimately altering the expression patterns of downstream genes. lncRNA, long non-coding RNA.

demonstrated that the alteration of linc01614 levels substantially affected β-catenin protein levels and WNT/β-catenin signaling.

*linc01614 combines with GSK-3β to stabilize the level of β-catenin protein*. To investigate the underlying mechanisms of linc01614 in the regulation of WNT/β-catenin signaling, RNA-pull down assays were conducted, followed by mass spectrometric analysis, in order to determine potential linc01614-interacting proteins in Panc-1 cells. A band between 43 and 55 kDa was specifically enriched in the linc01614 pull-down proteins and was subjected to mass spectrometry (Fig. 7A). GSK-3β, one of the key members of the WNT/β-catenin pathway, was identified as a potential linc01614-interacting protein (Fig. S3 and Table SVII). Bioinformatics analysis was then performed, to verify the potential interaction between linc01614 and GSK-3β in PC cells. By using the RPISeq database, it was observed that GSK-3β possessed a high interaction probability with linc01614 (Fig. 7B). The catRAPID database was used to predict possible binding sites between linc01614 and GSK-3β, and it was revealed that nucleotides 1471-1556 of the linc01614 sequence and amino acids 76-127 of the GSK-3β sequence were the most probable binding sites (Fig. 7C). Furthermore, western blot analysis revealed that GSK-3β was pulled down by biotin-labeled linc01614 transcript and not by linc01614 antisense (Fig. 7D). GSK-3β RIP assays in Panc-1 and SW1990 cells also revealed that linc01614 was markedly enriched by the anti-GSK-3β antibody (Fig. 7E). These results validated that linc01614 could possibly bind to GSK-3β.

Previous studies have demonstrated that AXIN1 can recruit GSK-3β, APC and CK1 to form a multi-protein degradation complex, which tightly regulates the degradation of β-catenin (32,33). The results of the present study also indicated that linc01614 can influence β-catenin expression at the post-transcriptional level (Fig. 6C and D). In addition, lncRNAs can restrict protein conformational shift or prevent the interaction among related proteins through binding (34,35). Hence, it was hypothesized that linc01614 perturbs the interaction between GSK-3β and AXIN1 through its binding to GSK-3β, thereby preventing the formation of the β-catenin degradation complex. In the present study, the results of Co-IP results confirmed that linc01614 knockdown enhanced the interaction between GSK-3β and AXIN1 (Fig. 7F and G), indicating that linc01614 negatively regulated the interaction between GSK-3β and AXIN1. Thus, linc01614 stabilized the level of β-catenin protein possibly through binding to GSK-3β, impeding the interaction between GSK-3β and AXIN1 (Fig. 8).

## Discussion

In the present study, it was identified that linc01614 was upregulated in PC. In PC cell lines, increased linc01614 expression was positively associated with tumor growth, invasiveness and migration. linc01614 functioned as a tumor promoter and obstruct the interaction between GSK-3β and AXIN1 by directly binding to GSK-3β, a vital protein of the WNT/β-catenin signaling pathway, thereby preventing the formation of the β-catenin degradation complex. Consequently, β-catenin may be accumulated in the cytoplasm and nucleus of PC cells, and the WNT/β-catenin pathway was activated. Therefore, the results illustrated the role and mechanism of linc01614 as an oncogene, activating the WNT/β-catenin pathway and promoting the progression of PC.

linc01614 is a 2,180 nucleotide-long intergenic non-protein coding RNA, encoded on the sense strand of chromosome 2. linc01614 is involved in the development of several

malignancies (16-21). These studies have mainly relied on bioinformatics analysis of linc01614 or its interaction with miRNAs as a competing endogenous RNA. However, whether linc01614 can perform a regulatory function by interacting with other cellular components (DNAs, RNAs and proteins) remains unclear. Additionally, the subcellular localization of a lncRNA inside the cell is crucial for understanding its functionality (36,37). FISH and subcellular fractionation assays confirmed that linc01614 was enriched in both PC cell cytoplasm and nucleus. This indicates that linc01614 may theoretically regulate fundamental cellular processes at different levels, including epigenetic modification, transcriptional, post-transcriptional, translational, and post-translational regulation. Of note, RNA pull-down and RIP assay demonstrated that linc01614 likely exerts its function by directly binding to GSK-3β, a vital protein of the canonical WNT/β-catenin pathway (38). Moreover, linc01614 disrupted the function of GSK-3β by affecting the interaction between GSK-3β and AXIN1 rather than reducing the translational production or increasing protein degradation. Hence, the present findings illustrated the molecular mechanisms of linc01614 in the progression of PC.

The canonical WNT signaling pathway controls the expression of critical developmental genes by regulating the accumulation of the transcriptional co-activator β-catenin. Aberrant WNT/β-catenin signaling has been previously implicated in PC (30,31,39). Moreover, lncRNAs may function as important signal transduction mediators in cancer signaling pathways, modifying cell fate and function (40-43). Based on bioinformatics analysis and experimental data, the present study successfully validated the linc01614-mediated activation of the WNT/β-catenin signaling pathway at the protein level in PC. Mechanistically, the scaffolding AXIN1 protein interacts with GSK3, CK1α and β-catenin at separate domains to form a β-catenin degradation complex. GSK-3β can phosphorylate the amino-terminal region of β-catenin, leading to subsequent β-catenin ubiquitination and proteasomal degradation (44). Therefore, β-catenin levels are possibly regulated by controlling GSK-3β activity in cells. It was revealed that linc01614 could interact with GSK-3β in PC; however, no significant differences in GSK-3β mRNA and protein levels between the control and linc01614 knockdown group were detected. However, the overexpression of linc01614 hindered the interaction between GSK-3β and AXIN1, thereby preventing the formation of the 'degradation complex' to degrade β-catenin.

Notably, GSK-3β itself participates in cell proliferation, apoptosis, cell cycle progression and cell signal transduction (45-47). As a serine-threonine kinase, GSK-3β can exert tumor-promoter and tumor-suppressor effects by phosphorylating a broad range of substrates (48,49). The function of GSK-3β in the onset and progression of PC and the acquisition of chemoresistance been previously established. For instance, the overexpression of GSK-3β can promote the invasive ability of Panc-1 cells by upregulating CXCR4 and MMP-2 expression (50). GSK-3β can also regulate cell cycle progression in cancer cells. In PC, GSK-3β can directly modulate the phosphorylation status of several cell cycle modulators, including cyclin D1 and p53 (51). Thus, GSK-3β may serve as a candidate therapeutic target for PC. Consistently, the present study revealed that LiCl, a GSK-3β inhibitor, upregulated the β-catenin level and subsequently promoted the progression of PC. Several lncRNAs, including MIR22HG and linc01197, have been reported to regulate the WNT/β-catenin signaling (40,52), whereas none of these lncRNAs bind to GSK-3β. However, considering the multiple biological functions of GSK-3β, the net effect of GSK-3β and the WNT/β-catenin pathway in PC still needs further analysis.

In conclusion, the present study demonstrated that linc01614 functioned as an oncogene and promoted the progression of PC. By binding to GSK-3β, linc01614 may stabilize the level of β-catenin protein to hyperactivate WNT/β-catenin signaling activity in PC. The current findings provide new insight into the underlying mechanisms of PC progression and a potential future therapeutic target for PC.

**Acknowledgements**

Not applicable.

**Funding**

The present study was supported by the Foundation of Health Commission of Hubei Province (grant nos. WJ2021M063, WJ2021F052).

**Availability of data and materials**

The datasets used and/or analyzed during the current study are available from the corresponding author on reasonable request.

**Authors' contributions**

ZGT and LJC conceived and designed the study. LJC and LW conducted most of the experiments with the assistance of WW and FX. LLZ and WBL analyzed the data. LJC wrote the first draft of the manuscript. ZGT performed critical revision and supervised all phases of the study. ZGT and LJC confirm the authenticity of all the raw data. All authors have read and approved the final manuscript.

**Ethical approval and consent to participate**

The present study was performed in accordance with the Declaration of Helsinki and approved by the Ethics Committee of Renmin Hospital of Wuhan University (approval no. WDRY2021-K188), and written informed consent was obtained from all subjects. All experiments were conducted according to the relevant guidelines and regulations and following the approval of the Institutional Animal Care Committee of Renmin Hospital of Wuhan University (approval no. WDRM20210606).

**Patient consent for publication**

Not applicable.

**Competing interests**

The authors declare that they have no competing interests.

## References


1. Siegel RL, Miller KD, Fuchs HE and Jemal A: Cancer statistics, 2021. CA Cancer J Clin 71: 7-33, 2021.
2. GBD 2017 Pancreatic Cancer Collaborators: The global, regional, and national burden of pancreatic cancer and its attributable risk factors in 195 countries and territories, 1990-2017: A systematic analysis for the global burden of disease study 2017. Lancet Gastroenterol Hepatol 4: 934-947, 2019.
3. Herting CJ, Karpovsky I and Lesinski GB: The tumor microenvironment in pancreatic ductal adenocarcinoma: Current perspectives and future directions. Cancer Metastasis Rev 40: 675-689, 2021.
4. Ho WJ, Jaffee EM and Zheng L: The tumour microenvironment in pancreatic cancer-clinical challenges and opportunities. Nat Rev Clin Oncol 17: 527-540, 2020.
5. Jarroux J, Morillon A and Pinskaya M: History, discovery, and classification of lncRNAs. Adv Exp Med Biol 1008: 1-46, 2017.
6. Liu S, Zhan N, Gao C, Xu P, Wang H, Wang S, Piao S and Jing S: Long noncoding RNA CBR3-AS1 mediates tumorigenesis and radiosensitivity of non-small cell lung cancer through redox and DNA repair by CBR3-AS1/miR-409-3p/SOD1 axis. Cancer Lett 526: 1-11, 2022.
7. Sun Y, Tian Y, He J, Tian Y, Zhang G, Zhao R, Zhu WJ and Gao P: Linc01133 contributes to gastric cancer growth by enhancing YES1-dependent YAP1 nuclear translocation via sponging miR-145-5p. Cell Death Dis 13: 51, 2022.
8. Hu H, Wang Y, Ding X, He Y, Lu Z, Wu P, Tian L, Yuan H, Liu D, Shi G, *et al*: Long non-coding RNA XLOC_000647 suppresses progression of pancreatic cancer and decreases epithelial-mesenchymal transition-induced cell invasion by down-regulating NLRP3. Mol Cancer 17: 18, 2018.
9. Singh N, Ramnarine VR, Song JH, Pandey R, Padi SK, Nouri M, Olive V, Kobelev M, Okumura K, Mccarthy D, *et al*: The long noncoding RNA H19 regulates tumor plasticity in neuroendocrine prostate cancer. Nat Commun 12: 7349, 2021.
10. Kopp F and Mendell JT: Functional classification and experimental dissection of long noncoding RNAs. Cell 172: 393-407, 2018.
11. Wang KC and Chang HY: Molecular mechanisms of long noncoding RNAs. Mol Cell 43: 904-914, 2011.
12. Gandhi M, Groß M, Holler JM, Coggins SA, Patil N, Leupold JH, Munschauer M, Schenone M, Hartigan CR, Allgayer H, *et al*: The lncRNA lincNMR regulates nucleotide metabolism via a YBX1-RRM2 axis in cancer. Nat Commun 11: 3214, 2020.
13. Iyer MK, Niknafs YS, Malik R, Singhal U, Sahu A, Hosono Y, Barrette TR, Prensner JR, Evans JR, Zhao S, *et al*: The landscape of long noncoding RNAs in the human transcriptome. Nat Genet 47: 199-208, 2015.
14. Livak KJ and Schmittgen TD: Analysis of relative gene expression data using real-time quantitative PCR and the 2(-Delta Delta C(T)) method. Methods 25: 402-408, 2001.
15. Pan S, Deng Y, Fu J, Zhang Y, Zhang Z and Qin X: N6-methyladenosine upregulates miR181d5p in exosomes derived from cancer associated fibroblasts to inhibit 5FU sensitivity by targeting NCALD in colorectal cancer. Int J Oncol 60: 14, 2022.
16. Chen Y, Cheng WY, Shi H, Huang S, Chen H, Liu D, Xu W, Yu J and Wang J: Classifying gastric cancer using FLORA reveals clinically relevant molecular subtypes and highlights linc01614 as a biomarker for patient prognosis. Oncogene 40: 2898-2909, 2021.
17. Vishnubalaji R, Shaath H, Elkord E and Alajez NM: Long non-coding RNA (lncRNA) transcriptional landscape in breast cancer identifies linc01614 as non-favorable prognostic biomarker regulated by TGFβ and focal adhesion kinase (FAK) signaling. Cell Death Discov 5: 109, 2019.
18. Liu AN, Qu HJ, Yu CY and Sun P: Knockdown of linc01614 inhibits lung adenocarcinoma cell progression by up-regulating miR-217 and down-regulating FOXP1. J Cell Mol Med 22: 4034-4044, 2018.
19. Sun Y and Ling C: Analysis of the long non-coding RNA linc01614 in non-small cell lung cancer. Medicine (Baltimore) 98: e16437, 2019.
20. Cai Q, Zhao X, Wang Y, Li S, Wang J, Xin Z and Li F: linc01614 promotes osteosarcoma progression via miR-520a-3p/SNX3 axis. Cell Signal 83: 109985, 2021.
21. Tang L, Chen Y, Peng X, Zhou Y, Jiang H, Wang G and Zhuang W: Identification and validation of potential pathogenic genes and prognostic markers in ESCC by integrated bioinformatics analysis. Front Genet 11: 521004, 2020.
22. Aiello NM, Brabletz T, Kang Y, Nieto MA, Weinberg RA and Stanger BZ: Upholding a role for EMT in pancreatic cancer metastasis. Nature 547: E7-E8, 2017.
23. Thiery JP: Epithelial-mesenchymal transitions in tumour progression. Nat Rev Cancer 2: 442-454, 2002.
24. Wang L, Wu H, Wang L, Zhang H, Lu J, Liang Z and Liu T: Asporin promotes pancreatic cancer cell invasion and migration by regulating the epithelial-to-mesenchymal transition (EMT) through both autocrine and paracrine mechanisms. Cancer Lett 398: 24-36, 2017.
25. Liu Y, Tang T, Yang X, Qin P, Wang P, Zhang H, Bai M, Wu R and Li F: Tumor-derived exosomal long noncoding RNA LINC01133, regulated by Periostin, contributes to pancreatic ductal adenocarcinoma epithelial-mesenchymal transition through the Wnt/β-catenin pathway by silencing AXIN2. Oncogene 40: 3164-3179, 2021.
26. Zhang J, Cai H, Sun L, Zhan P, Chen M, Zhang F, Ran Y and Wan J: LGR5, a novel functional glioma stem cell marker, promotes EMT by activating the Wnt/β-catenin pathway and predicts poor survival of glioma patients. J Exp Clin Cancer Res 37: 225, 2018.
27. Liu SL, Cai C, Yang ZY, Wu ZY, Wu XS, Wang XF, Dong P and Gong W: DGCR5 is activated by PAX5 and promotes pancreatic cancer via targeting miR-3163/TOP2A and activating Wnt/β-catenin pathway. Int J Biol Sci 17: 498-513, 2021.
28. Ram Makena M, Gatla H, Verlekar D, Sukhavasi S, K Pandey M and C Pramanik K: Wnt/β-Catenin signaling: The culprit in pancreatic carcinogenesis and therapeutic resistance. Int J Mol Sci 20: 4242, 2019.
29. Tang N, Xu S, Song T, Qiu Y, He J and Fu X: Zinc finger protein 91 accelerates tumour progression by activating β-catenin signalling in pancreatic cancer. Cell Prolif 54: e13031, 2021.
30. Wang L, Heidt DG, Lee CJ, Yang H, Logsdon CD, Zhang L, Fearon ER, Ljungman M and Simeone DM: Oncogenic function of ATDC in pancreatic cancer through Wnt pathway activation and beta-catenin stabilization. Cancer Cell 15: 207-219, 2009.
31. Zhou C, Liang Y, Zhou L, Yan Y, Liu N, Zhang R, Huang Y, Wang M, Tang Y, Ali DW, *et al*: TSPAN1 promotes autophagy flux and mediates cooperation between WNT-CTNNB1 signaling and autophagy via the MIR454-FAM83A-TSPAN1 axis in pancreatic cancer. Autophagy 17: 3175-3195, 2021.
32. Kishida S, Yamamoto H, Ikeda S, Kishida M, Sakamoto I, Koyama S and Kikuchi A: Axin, a negative regulator of the wnt signaling pathway, directly interacts with adenomatous polyposis coli and regulates the stabilization of beta-catenin. J Biol Chem 273: 10823-10826, 1998.
33. Seeling JM, Miller JR, Gil R, Moon RT, White R and Virshup DM: Regulation of beta-catenin signaling by the B56 subunit of protein phosphatase 2A. Science 283: 2089-2091, 1999.
34. Jiang M, Zhang S, Yang Z, Lin H, Zhu J, Liu L, Wang W, Liu S, Liu W, Ma Y, *et al*: Self-recognition of an inducible host lncRNA by RIG-I feedback restricts innate immune response. Cell 173: 906-919, 2018.
35. Xu J, Shao T, Song M, Xie Y, Zhou J, Yin J, Ding N, Zou H, Li Y and Zhang J: MIR22HG acts as a tumor suppressor via TGFβ/SMAD signaling and facilitates immunotherapy in colorectal cancer. Mol Cancer 19: 51, 2020.
36. Cabili MN, Dunagin MC, Mcclanahan PD, Biaesch A, Padovan-Merhar O, Regev A, Rinn JL and Raj A: Localization and abundance analysis of human lncRNAs at single-cell and single-molecule resolution. Genome Biol 16: 20, 2015.
37. van Heesch S, van Iterson M, Jacobi J, Boymans S, Essers PB, De Bruijn E, Hao W, Macinnes AW, Cuppen E and Simonis M: Extensive localization of long noncoding RNAs to the cytosol and mono- and polyribosomal complexes. Genome Biol 15: R6, 2014.
38. Li Q, Sun M, Wang M, Feng M, Yang F, Li L, Zhao J, Chang C, Dong H, Xie T, *et al*: Dysregulation of Wnt/β-catenin signaling by protein kinases in hepatocellular carcinoma and its therapeutic application. Cancer Sci 112: 1695-1706, 2021.
39. Morris JP IV, Wang SC and Hebrok M: KRAS, Hedgehog, Wnt and the twisted developmental biology of pancreatic ductal adenocarcinoma. Nat Rev Cancer 10: 683-695, 2010.
40. Han M, Wang S, Fritah S, Wang X, Zhou W, Yang N, Ni S, Huang B, Chen A, Li G, *et al*: Interfering with long non-coding RNA MIR22HG processing inhibits glioblastoma progression through suppression of Wnt/β-catenin signalling. Brain 143: 512-530, 2020.

41. Nyati KK, Hashimoto S, Singh SK, Tekguc M, Metwally H, Liu YC, Okuzaki D, Gemechu Y, Kang S and Kishimoto T: The novel long noncoding RNA AU021063, induced by IL-6/Arid5a signaling, exacerbates breast cancer invasion and metastasis by stabilizing Trib3 and activating the Mek/Erk pathway. Cancer Lett 520: 295-306, 2021.
42. Wu N, Jiang M, Liu H, Chu Y, Wang D, Cao J, Wang Z, Xie X, Han Y and Xu B: LINC00941 promotes CRC metastasis through preventing SMAD4 protein degradation and activating the TGF-β/SMAD2/3 signaling pathway. Cell Death Differ 28: 219-232, 2021.
43. Xu M, Cui R, Ye L, Wang Y, Wang X, Zhang Q, Wang K, Dong C, Le W and Chen B: LINC00941 promotes glycolysis in pancreatic cancer by modulating the Hippo pathway. Mol Ther Nucleic Acids 26: 280-294, 2021.
44. Kimelman D and Xu W: beta-catenin destruction complex: Insights and questions from a structural perspective. Oncogene 25: 7482-7491, 2006.
45. Ryu HY, Kim LE, Jeong H, Yeo BK, Lee JW, Nam H, Ha S, An HK, Park H, Jung S, *et al*: GSK3B induces autophagy by phosphorylating ULK1. Exp Mol Med 53: 369-383, 2021.
46. Park R, Coveler AL, Cavalcante L and Saeed A: GSK-3β in pancreatic cancer: Spotlight on 9-ING-41, its therapeutic potential and immune modulatory properties. Biology (Basel) 10: 610, 2021.
47. Zhang Z, Gao Q and Wang S: Kinase GSK3β functions as a suppressor in colorectal carcinoma through the FTO-mediated MZF1/c-Myc axis. J Cell Mol Med 25: 2655-2665, 2021.
48. Duda P, Akula SM, Abrams SL, Steelman LS, Martelli AM, Cocco L, Ratti S, Candido S, Libra M, Montalto G, *et al*: Targeting GSK3 and associated signaling pathways involved in cancer. Cells 9: 1110, 2020.
49. Pecoraro C, Faggion B, Balboni B, Carbone D, Peters GJ, Diana P, Assaraf YG and Giovannetti E: GSK3β as a novel promising target to overcome chemoresistance in pancreatic cancer. Drug Resist Updat 58: 100779, 2021.
50. Ying X, Jing L, Ma S, Li Q, Luo X, Pan Z, Feng Y and Feng P: GSK3β mediates pancreatic cancer cell invasion in vitro via the CXCR4/MMP-2 pathway. Cancer Cell Int 15: 70, 2015.
51. Mccubrey JA, Rakus D, Gizak A, Steelman LS, Abrams SL, Lertpiriyapong K, Fitzgerald TL, Yang LV, Montalto G, Cervello M, *et al*: Effects of mutations in Wnt/β-catenin, hedgehog, Notch and PI3K pathways on GSK-3 activity-diverse effects on cell growth, metabolism and cancer. Biochim Biophys Acta 1863: 2942-2976, 2016.
52. Ling J, Wang F, Liu C, Dong X, Xue Y, Jia X, Song W and Li Q: FOXO1-regulated lncRNA LINC01197 inhibits pancreatic adenocarcinoma cell proliferation by restraining Wnt/β-catenin signaling. J Exp Clin Cancer Res 38: 179, 2019.